| Journal of Coastal Research | SI | 94 | 362–366 | Coconut Creek, Florida | 2019 |
|---|---|---|---|---|---|

# Computer Analysis of Influence of Moisture Content of the Fine-Silty Sand for the CEP Pile Applied for Oceanographic Engineering under Vertical Tensile

**Yongmei Qian[†*], Hongbin Liu[†], Xinsheng Yin[†], and Yujie Jin[†]**

[†]Jilin Jianzhu University
Changchun 130118, China

www.cerf-jcr.org

www.JCRonline.org

**ABSTRACT**

Qian, Y.-M.; Liu, H.-B.; Yin, X.-S., and Jin, Y.-J., 2019. Computer analysis of influence of moisture content of the fine-silty sand for the CEP pile applied for oceanographic engineering under vertical tensile. *In:* Gong, D.; Zhu, H., and Liu, R. (eds.), *Selected Topics in Coastal Research: Engineering, Industry, Economy, and Sustainable Development*. *Journal of Coastal Research*, Special Issue No. 94, pp. 362–366. Coconut Creek (Florida), ISSN 0749-0208.

In oceanographic engineering, it is the most important factor of the bearing capacity of pile, which is the function of the CEP pile. This paper takes the concrete expanded-plates pile (CEP pile) as the research object, and conducts theoretical analysis on the influence of the moisture content of fine-salty sand towards its uplift bearing capacity and the failure state of the soil around the pile. By conducting simulation using the ANSYS finite element software, this paper analyzes the displacement, stress, strain of the CEP pile and other results under different moisture contents, so as to determine the optimal moisture content for setting bearing plates in the fine-silty sand, and to provide reliable theoretical basis for the reasonable design and application of the CEP pile.

**ADDITIONAL INDEX WORDS:** *Vertical tensile, concrete expanded-plates pile (CEP pile), fine-silty sand, moisture content, simulation analysis.*

## INTRODUCTION

As a new type of non-uniform pile, the CEP pile has the advantages of reducing foundation settlement and saving costs (Wang, He, and Tang, 2008). The theoretical research on the application of the CEP pile in the cohesive soil with high bearing capacity has been gradually perfected (Qian *et al*., 2005). However, during actual construction, in some geo-environment, the cohesive soil layers are too thin, or there is no cohesive soil that meets the design requirements of the bearing capacity (Wang, Cheng, and Wang, 2013). Under these conditions, the bearing plate of the CEP pile may be placed in the non-cohesive soil layer, including silty soil, fine-silty sand and so on, which will affect the mechanical properties of the concrete pile. At this stage, the research on the bearing capacity of CEP pile and the influencing factors of the soil failure state are mainly focused on the pile itself. However, the relevant parameters of the soil mass around the pile also have nonnegligible effects on the ultimate bearing capacity of the pile, for instance, soil mass moisture content, density and so on, and these influencing factors are not reflected in the current calculation formula of the ultimate bearing capacity of the single CEP pile (Sun and Wang, 2010).

The actual experience shows that when the soil moisture content around the pile is large, as the load on pile-top increases, the bearing capacity of the pile decreases and the vertical displacement increases, punch failure is likely to occur to the soil around the pile. On the contrary, when the moisture content is low, the bearing capacity of CEP pile is large, therefore, further studies of the influence of soil moisture content around the pile on the bearing capacity of concrete pile need to be conducted. This paper uses ANSYS finite element to construct the model and conduct analysis, studies the impact of fine-salty sand moisture content on the bearing capacity of the expanded-plates pile and the soil failure state around the pile when the pile is in fine-salty sand and under vertical tensile, then the paper draws a theoretical basis for guiding practice (Chen *et al*., 2014; Palsania *et al*., 2008; Yin, Jia, and Ding, 2018).

## FINITE ELEMENT MODEL ESTABLISHMENT

### Concrete Unit Type and Material Properties Definition

This paper still takes the half section pile as the object for analysis, when building the soil-pile model (Qian and Wang, 2015) by ANSYS software, it uses the SOLID65 entity unit type to stimulate the CEP pile and its surrounding soil mass. SOLID65 is a 3-D reinforced concrete unit built on the basis of SOLID45 unit, taking into account the properties of the concrete. It is mainly used to simulate unreinforced or reinforced entity structures which would crack under tensile and crash under compression. The unit is defined by eight nodes, each node has three degrees of freedom, namely, the translational displacements along the x, y, and z directions of the nodes coordinates. It is the same as the actual situation and can simulate and analysis the soil mass around the pile ideally (Du *et al*., 2016; Ye, Wang and Gan, 2016; Zhang *et al*., 2013).

To ensure the material properties of the simulated unit are consistent with the parameters of the later experimental study, this paper refers to the relevant data and sets the physical properties of the concrete and the fine-salty sand, as shown in Table 1.

*DOI: 10.2112/SI94-074.1 received 2 February 2019; accepted in revision 5 Month 2019.*
*Corresponding author: 654675316@qq.com

Table 1. *The material properties of the concrete and the fine-silty sand.*

| Material | Elastic Modulus (*Mpa*) | Unit weight ($kg/mm^3$) | Poisson's ratio | Friction coefficient |
|---|---|---|---|---|
| Concrete | 2.5E4 | 2.5E-6 | 0.2 | 0.3 |
| sand | 30 | 1.95E-6 | 0.25 | 0.3 |

## Parameter Settings for Different Model Groups of Ansys Finite Element

In ANSYS, the yield surface of the Drucker-Prager (or DP model for short) failure criterion does not change with the yield state of the material, and its constitutive model uses the ideal elastoplastic model. The criterion can be expressed as:

$$\sigma_e = 3\beta\sigma_m + \sqrt{\frac{1}{2}\{S\}^T[M]\{S\}} = \sigma_y \quad (1)$$

where, {S} is the deviatoric stress; $\sigma_m$=1/3($\sigma_x$+$\sigma_y$+$\sigma_z$) is the average stress; [M] is a constant coefficient matrix.The yield strength σ of the material is given by:

$$\sigma_y = \frac{6c\cos\varphi}{\sqrt{3}(3-\sin\varphi)} \quad (2)$$

where, c is the cohesion of the material; $\Phi$ is the angle of internal friction of the material.

In the simulation analysis, make sure other conditions remain unchanged, and control the moisture content of the fine-salty sand as a single variable. Select the simulated moisture content in turn as: 17.5%, 15.89%, 14.5%, 13.6%, 12.5%, 11.61%, 10.5% and 9.94%, divided into eight groups of models and named MC1-MC8; according to the relationship between moisture content of fine-salty sand and shear strength, we can calculate shear strength indexes for corresponding moisture content of fine-salty sand, as shown in Table 2. DP failure criterion is used in the input of relevant parameters (Bian *et al*., 2016; 2017).

## Model Construction and Mesh Generation

This paper combines the actual size of the CEP pile in the previous experiment, when using ANSYS finite element to construct the model, it sets the soil mass around the pile into column shape with a radius of 5000 mm. The height of the whole soil mass was set to 8000 mm. The CEP pile is set at 1800 mm from the bottom of the soil mass, and the upper part reserves 6200 mm. The CEP pile and surrounding soil mass are divided in a mapping mesh type, the shape of each unit is a hexahedron cell, and denser division is conducted around the expanded-plates.

## Pile-Soil Contact Surface Treatment and Model Loading

In order to effectively simulate the contact and slippage state between the pile body and the soil mass around the pile, the contact surface of the two was modeled by the two element types of CONTA174 and TARGE170 in the simulation analysis by ANSYS. In addition, as the bottom of CEP pile touches the soil layer, 10mm separation is reserved and a 10mm gap is also reserved between the expanded-plate lower boundary and the soil mass, namely the non-contact surface, as shown in Figure 1.

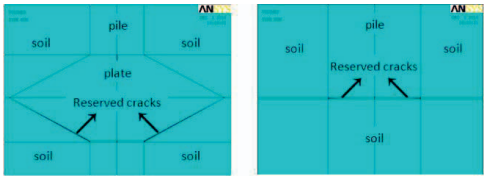


Figure 1. The reserved separation of the CEP pile and soil mass.

Before loading the model, the boundary conditions of the model need to be controlled. The main constraints are the three degrees of freedom of translation, that is to restrain from three directions x, y and z, respectively, impose vertical restrain on the front of the half section pile including the soil mass; impose vertical restrain on the entire soil mass bottom, including the bottom of the CEP pile; and impose restrain from three directions on the outer circular surface of the soil mass. When loading the model, apply the surface load evenly to the upper part of the semicircular surface of the half section pile, in straight up direction. Start the loading from 50 KN and gradually increase the loading by 50 KN, according to formula $P$=$F/A$, the concentrated load is converted into the surface load, that is to start loading from 0.5 N/mm$^2$ and gradually increase the loading by 0.5 N/mm$^2$ each time.

# ANSYS FINITE ELEMENT LOAD-DISPLACEMENT RESULT ANALYSIS

## ANSYS Finite Element Displacement Nephogram of Different Model Groups

Through the establishment of the above ANSYS finite element model and loading calculation, the Y-direction displacement nephogram of MC1-MC8 pile soil is obtained, as shown in Figure 2.

After analyzing the displacement nephogram of the various finite element models of MC1-MC8, it can be found that when the moisture content of fine-salty sand decreases, the Y-direction displacement of the CEP pile gradually decreases, which further indicates that the bearing capacity increases gradually. From MC3 to MC8, the Y-direction displacement of these six groups of models did not change much, but the Y-direction displacement of the two models of MC1 and MC2 changed a lot, which indicated that in the two cases of fine-salty sand with moisture content of 17.5% and 15.89%, the bearing capacity of the CEP pile is low. When the moisture content of

Table 2. *The groups of ANSYS finite element model and the corresponding shear strength indexes.*

| | MC1 | MC2 | MC3 | MC4 | MC5 | MC6 | MC7 | MC8 |
|---|---|---|---|---|---|---|---|---|
| Moisture content (%) | 17.5 | 15.89 | 14.5 | 13.6 | 12.5 | 11.61 | 10.5 | 9.94 |
| Cohesion (KPa) | 29.01 | 34.11 | 38.52 | 41.37 | 3.47 | 45.2 | 46.97 | 47.96 |
| Angle of internal friction (°) | 28.88 | 31.9 | 34.51 | 36.2 | 36.8 | 37.3 | 39.56 | 40.7 |

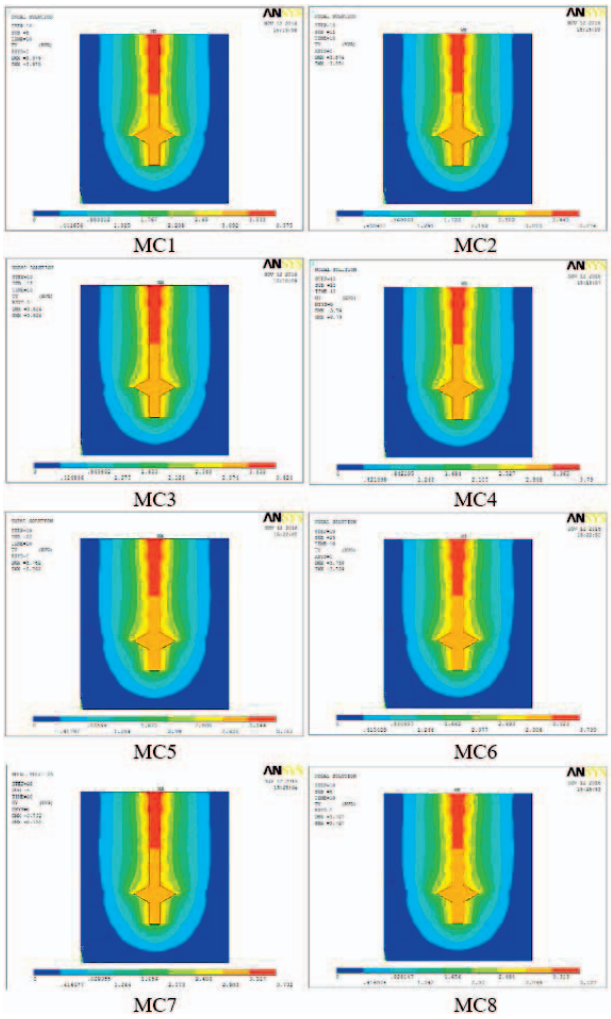


Figure 2. Y-direction pile soil displacement under different moisture content of fine-salty sand.

the fine-salty sand is lower than 14.5%, the bearing capacity of the CEP pile is higher.

### Load-Displacement Curves of Ansys Finite Element Model Groups

In the process of ANSYS finite element calculation, when the applied vertical load on the top of MC1 model reaches 500 KN, the model was immediately damaged. Therefore, from the MC1-MC8 eight groups of models, one-by-one taking the center point of the CEP pile-top as the research object, the pile top load was applied from 50 KN to 500 KN, under each load step, there's responding Y-direction displacement data which were sorted out to obtain the rule of Y-direction displacement with load changes of a fixed point of the pile-top of each model, then the load-displacement curve at a fixed point on the top of MC1-MC8 model was drawn as shown in Figure 3.

Analysis of the model's load-displacement curve in Figure 3 leads to the following conclusion:

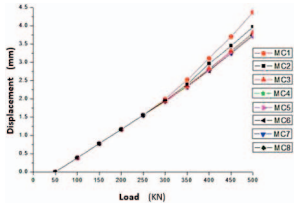


Figure 3. The load-displacement curves of MC1-MC8 models.

(1) The trend of load-displacement curve of each model is roughly the same, that is, the vertical displacement of CEP pile-top gradually increases with the increase of vertical load.
(2) During the whole loading process, the vertical displacement of pile-top of MC3-MC8 model basically remains the same. When the loading was in the range of 0-300KN, the MC1 model and MC2 model are the same with MC3-MC8 in the vertical displacement of pile-top; but when the vertical load exceeds 300 KN, the rate of increase of pile-top vertical displacement is obviously higher than that of MC3-MC8 model, and the mutation occurs. The result shows that when the moisture content of fine-salty sand is higher than 15%, the bearing capacity of CEP pile is obviously lower than that of other models.
(3) It is found through comparison that when the vertical loads on the top of CEP pile are the same, the maximum vertical displacement of pile-top is the MC1 model, and the minimum is MC8 model. When the vertical displacement of CEP pile is the same, the CEP pile with the highest bearing capacity is MC8 model, and the lowest is MC1 model; it indicates that with the decrease of fine-salty sand moisture content, the vertical displacement of CEP pile becomes smaller, and the bearing capacity becomes better.

## ANSYS FINITE ELEMENT STRESS-STRAIN RESULT ANALYSIS

### ANSYS Finite Element Stress Analysis

#### (1) Y-direction stress nephogram analysis of models with different moisture content

During ANSYS post-processing, we can extract the Y-direction stress nephogram of MC1-MC8 models under the same vertical load as shown in Figure 4.

After analyzing the Y-direction stress nephogram of the MC1-MC8 models, it can be found that under the same vertical load, the maximum Y-stress of the eight groups of models appears at the top of the model pile, and the stress decreases from the pile-top to the pile-bottom, the stress value in the Y-direction under the bearing plate is very small, while the stress value in the Y-direction at the upper and lower regions of the bearing plate changes obviously. When the vertical tensile of the model pile-top are the same, the stress in Y-direction gradually decreases, that is, as the moisture content of fine-salty sand around the pile gradually decreases, the Y-direction

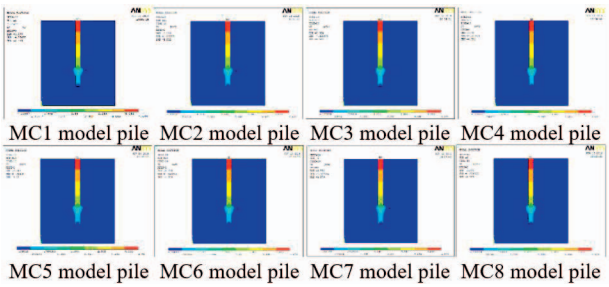


Figure 4. The Y-direction stress nephogram of MC1-MC8 models.

stress of the pile gradually decreases as well, but the difference was not significant.

**(2) XY-direction shear stress curve analysis of model pile with different moisture content**

In order to further understand the trend of XY-direction shear stress variation of MC1-MC8 model piles, in the MC1-MC8 models, several nodes were evenly extracted from the pile-top to the pile-bottom, then we sorted out XY-direction shear stress of the nodes under the same load and drew curves as shown in Figure 5.

Analysis of the curves in Figure 6 shows that the shear stress values of the MC1-MC8 model piles are obviously changed at the upper and lower inflection points of the bearing expanded-plate, and the maximum shear stress appears at the position of the bearing plate. In upper part of the model pile expanded-plate, the shear stress changes little along the pile body, while in lower part, the shear stress changes obviously, the value of shear stress increases from plate bottom to the pile bottom. For the expanded plate, the shear stress of upper part of the pile is obviously smaller than that of the lower part of the pile. In addition, when the moisture content of fine-salty sand is different, the trend of shear stress change of the eight model piles is basically the same under the same vertical tensile of the CEP pile, this further indicates that, the moisture content of fine-salty sand around the CEP pile has little effect on the shear stress of the pile body (Hu *et al*., 2017).

**(3) XY-direction shear stress curve analysis of the soil mass around model piles with different moisture content**

Along the pile-top to the pile-bottom, evenly pick points of the soil mass around the pile, then extract XY-direction shear

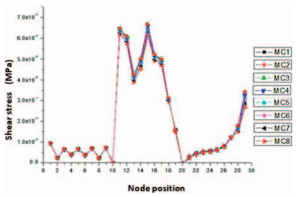


Figure 5. Shear stress curves of MC1-MC8 model piles in the fine-salty sand.

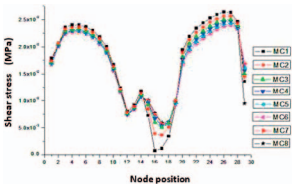


Figure 6. The shear stress curves of the soil around the MC1-MC8 model piles in the fine-salty sand. *Note: In the figure, the abscissa represents the position of the node, 1-10 represent node positions in upper part of model pile, 20-29 represent node positions in lower part of model piles, 11 represents the inflection point in upper part of the expanded-plate, 19 represents the inflection point in lower part of the expanded-plate, 15 represents the top point of the expanded-plate*.

stress values of the soil mass around the MC1-MC8 model piles to draw curves and make comparison as shown in Figure 6.

Through the analysis we can see that: overall, for the shear stress curve of soil mass around the MC1-MC8 model piles, its curve is basically parabola and symmetrical to the top point of the bearing expanded-plate. When the vertical tension of the model pile-top is the same, and the moisture content of fine-salty sand around the model piles is different, the shear stress curve of the soil mass above the bearing expanded-plate is basically consistent. In summary, when the moisture content of fine-salty sand exceeds 15%, the XY-direction shear stress of the soil mass around the pile is extremely small at the bearing expanded-plate and is extremely large at the lower part of the plate, and the range of the mutation is quite obvious. When the moisture content is less than 15%, the XY-direction shear stress curve of the soil mass around the model piles are basically the same (Liu, Xu, and Zhou, 2018).

## ANSYS Finite Element Model Strain Result Analysis

During the ANSYS post-processing, extract the Y-direction total strain contours of the MC1-MC8 eight groups of models when the vertical tensile of pile-top are all 500 KN, as shown in Figure 7. In the contour figure, A-I in turn represents the model's gradual change from small to large of the total strain in Y-direction, the density degree of the contour marks is set at 4.

From the analysis of the total strain contour in Figure 7, it can be concluded that, in the bottom part of the CEP pile, the strain near the pile-end is the largest, then decreases along the two sides of the pile-end, and is axisymmetric to the pile body.

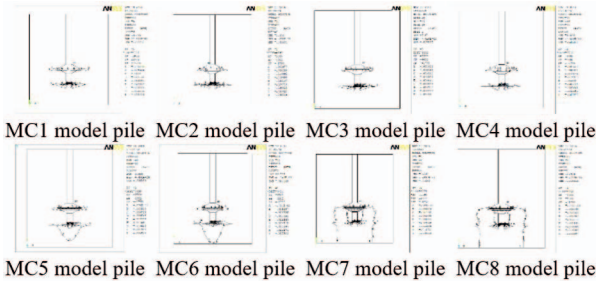


Figure 7. The Y-direction total strain contour of the MC1-MC8 models.

For MC1-MC8 models, all the Y-direction total strain maximums appear at the bottom of the CEP pile, while the lower part of the expanded-plate also has smaller strain; at the same time, as the moisture content of the soil mass around the pile decreases, the strains of MC1-MC3 models are basically the same, about 0.046 MPa, while the Y-direction strain of MC4 model is about 0.039 MPa. For MC4-MC8 models, the rate of strain decrease slows down, so the moisture content of the fine-salty sand around the CEP pile is better not higher than 15% (Wang *et al*., 2018).

## CONCLUSION

When the moisture content of fine-salty sand around the pile is higher than 15%, the pile-top displacement of the CEP pile is larger and the bearing capacity is worse. When the moisture content of fine-salty sand is below 15%, as the decrease of fine-salty sand moisture content, the vertical displacement of CEP pile becomes smaller, and the carrying capacity is better.

The moisture content of fine-salty sand has little effect on the Y-direction stress of CEP pile, but due to the existence of bearing expanded-plate pile, the shear stress near the expanded-plate of the CEP pile is higher than that of the upper or lower part of the pile body of the plate, and when the moisture content of fine-salty sand is higher than 15%, the shear stress of soil mass around the pile near the expanded-plate is smaller, indicating that the soil mass around the expanded-plate has better plasticity.

When the moisture content of fine-salty sand is higher than 15%, the total strain of the model in the Y-direction is larger, and as the moisture content of fine-salty sand decreases, the Y-direction total strain decreases more slowly. Therefore, setting bearing plate in the fine-salty sand with less than 15% moisture content will achieve a good effect.

## ACKNOWLEDGMENTS

This work was financially supported by National Natural Science Foundation of China (51678275 and 51278224).

## LITERATURE CITED

Bian, X.; Ca, B.; Zhi, X., and Cao, Y., 2016. Compressibility of cemented dredged clay at high water content with super-absorbent polymer. *Engineering Geology*, 208, 198-205.

Bian, X.; Ding, G.; Wang, Z.; Cao, Y., and Ding, J., 2017. Compression and strength behavior of cement-lime-polymer-solidified dredged material at high water content. *Marine Georesources & Geotechnology*, 35, 840-846.

Chen, S.; Guo, W.J.; Zhou, H.; Shen, B., and Liu, J., 2014. Field investigation of long-term bearing capacity of strip coal pillars. *International Journal of Rock Mechanics and Mining Sciences*, 70, 109-114.

Du, Y.; Song, C.; Chen, L., and Yang, J., 2016. PS wave based parallel seismic test for pile length assessment. *Soils and Foundations*, 56, 440-448.

Fan, A.; Yang, R.; Lenhardt, N.; Wang, M.; Han, Z.; Li, J.; Li, Y., and Zhao, Z., 2019. Cementation and porosity evolution of tight sandstone reservoirs in the Permian Sulige gas field, Ordos Basin (central China), *Marine and Petroleum Geology*, 103, 267-293.

Hu, S.; Tan, Y.; Zhou, H.; Guo, W., and Hu, D., 2017. Impact of bedding planes on mechanical properties of sandstone. *Rock Mechanics and Rock Engineering*, 50, 2243-2251.

Liu, Y.; Xu, J., and Zhou, G., 2018. Relation between crack propagation and internal damage in sandstone during shear failure. *Journal of Geophysics and Engineering*, 15, 2104-2109.

Palsania, J.; Sharma, R.; Srivastava, J.K., and Sharma, D., 2008. Effect of moisture content variation over kinetic reaction rate during vermicomposting process. *Applied Ecology and Environmental Research*, 6, 91-93.

Qian, Y.M. and Wang, X.H., 2015. Finite element analysis of the compressive carrying capacity on influence of the plate space of the concrete expanded pile, *Industrial Construction*, 45, 997-999.

Qian, Y.M.; Yin, X.S.; Zhong, C.L., and Wang, R.-Z., 2005. Study on the ultimate bearing capacity of soil under multi-extruded-expanded-plates pile, *Journal of Harbin Institute of Technology*, 4, 568-570.

Sun, X.D. and Wang, D., 2010. Analysis of the value of cohesion of soil. *Liaoning Building Materials*, 3, 39-41.

Wang, M.S.; He, D.X., and Tang, S.T., 2008. New technology of pile foundation in 21st Century: Rotate to dig and squeeze the enlarged DX pouring pile. *Industrial Construction*, 38, 23-27.

Wang, Y.; Chen, Y.; Qiao, W.; Zuo, D., and Hu, Z., 2018. Road engineering field tests on an artificial crust layer combined with pre-stressed pipe piles over soft ground. *Soil Mechanics and Foundation Engineering*, 54, 402-408.

Wang, Y.L.; Cheng, Z.L., and Wang, Y., 2013. Effects of liquefaction-induced large lateral ground deformation on pile foundations, *Journal of Central South University*, 20, 2510-2518.

Ye, X.M.; Wang, Z., and Gan, F., 2016. Research on calculation method of anchoring and anti-slide piles based on displacement of soil around piles. *Journal of Rock Mechanics and Geotechnical Engineering*, s1, 3187-3194.

Yin, S.; Jia, Q., and Ding, W., 2018. 3D paleotectonic stress field simulations and fracture prediction for marine-continental transitional facies forming a tight-sandstone reservoir in a highly deformed area. *Journal of Geophysics and Engineering*, 15, 1214-1230.

Zhang, X.; Zhou, X.; Zhou, H.; Gao, X.; Gao,Z., and Wang, Z., 2013. Studies on forecasting of carbonation depth of slag high performance concrete considering gas permeability. *Applied Clay Science*, 79, 36-40.